Chapter 4 - Confinement

Hunt Feng[1]

[1]Faculty of Physics And Engineering Physics
University of Saskatchewan

October 6, 2023

Outline of Presentation

Outline of Presentation

Resistive Plasma Diffusion

- Resistive diffusion coefficient

$$D = \frac{\eta_\perp \beta}{2\mu_0} \sim \frac{\rho}{\tau} = D_c$$

  where ρ and τ are step length and step time from classical random walk model.
- Resistive diffusion gives diffusion coefficient similar to classical result D_c.

Banana/Plateau/Pfirsch-Schlüter Transport

- Classical diffusion coefficient is $D_c = \rho^2 \nu$, where ρ is the random walk length, and ν is the collision frequency.
- Plateau diffusion coefficient

$$D \sim \frac{v_{\|}}{v_T} v_d^2 \frac{Rq}{v_{\|}} \sim \frac{v_T q}{R} \rho^2$$

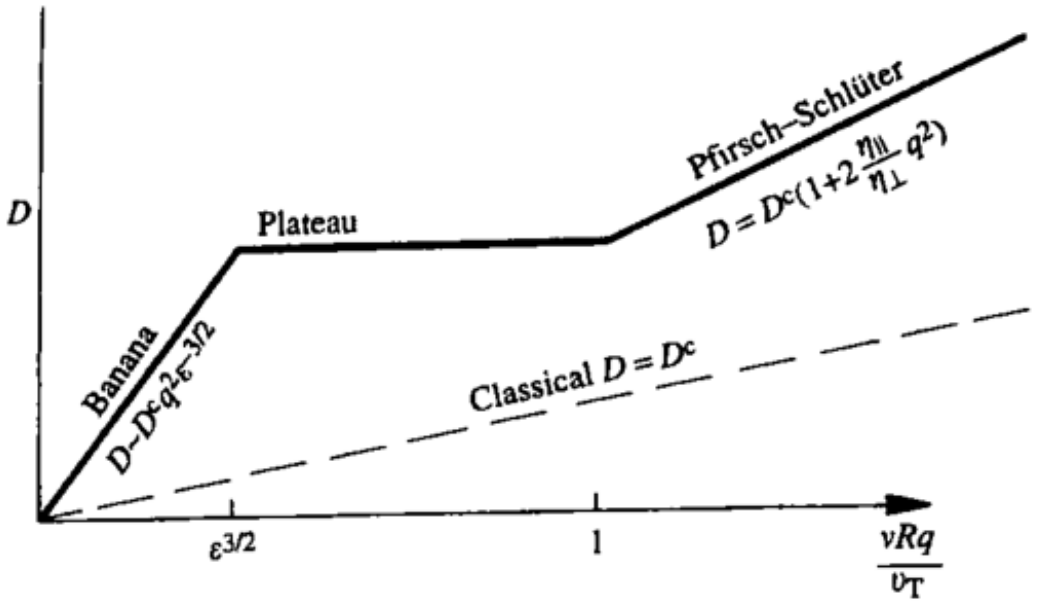

Figure 1: Variation of diffusion coefficient with collision frequency.

Ripple Transport

- The finite number of toroidal field coils destroys the perfect axisymmetry of the device.
- Particles are trapped / lose energies to the "ripple well".

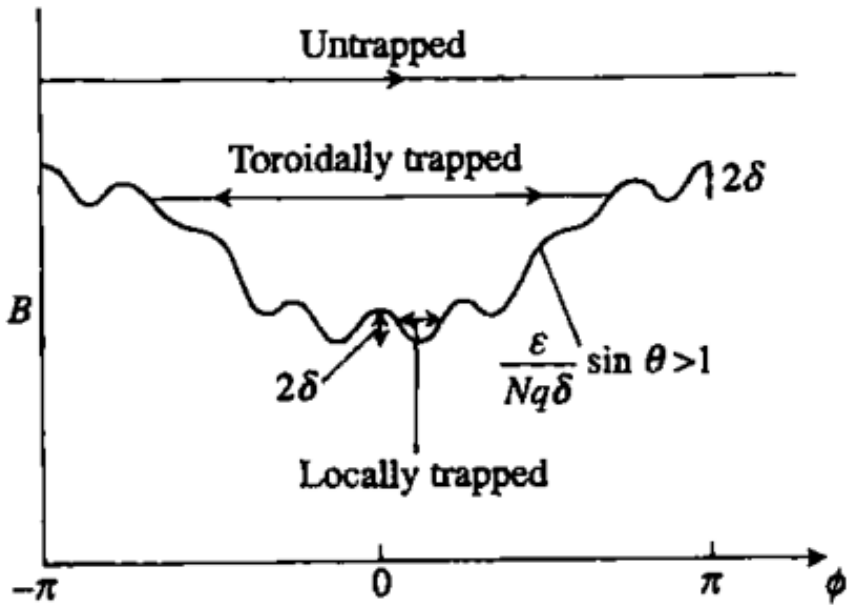

Figure 2: Variation of magnetic field strength along a field line in a tokamak with a rippled field, and the resulting types of particle trapping.

Outline of Presentation

Confinement Modes

- **Ohmically heated plasmas**:

$$\tau_E = 0.07(n/10^{20})aR^2q$$

Confinement increases as density increases.

- **L-mode**:

$$\tau_E^{ITER89-P} = 0.048\frac{I^{0.85}R^{1.2}a^{0.3}\kappa^{0.5}(n/10^{20})^{0.1}B^{0.2}A^{0.5}}{P^{0.5}}$$

Confinement drops and heating power P increases.

- **H-mode**:

$$\tau_{Th}^{ITERH93-P} = 0.053\frac{I^{1.06}R^{1.9}a^{-0.11}\kappa^{0.66}(n/10^{20})^{0.17}B^{0.32}A^{0.41}}{P^{0.67}}$$

τ_{Th} refers to confinement time for the thermal part of the plasma energy. It is valid without edge localized modes (ELMs).

H-modes

- H-mode has good confinement.
- At the edge, shape density gradient is steep.
- Transport barrier at the edge is developed.

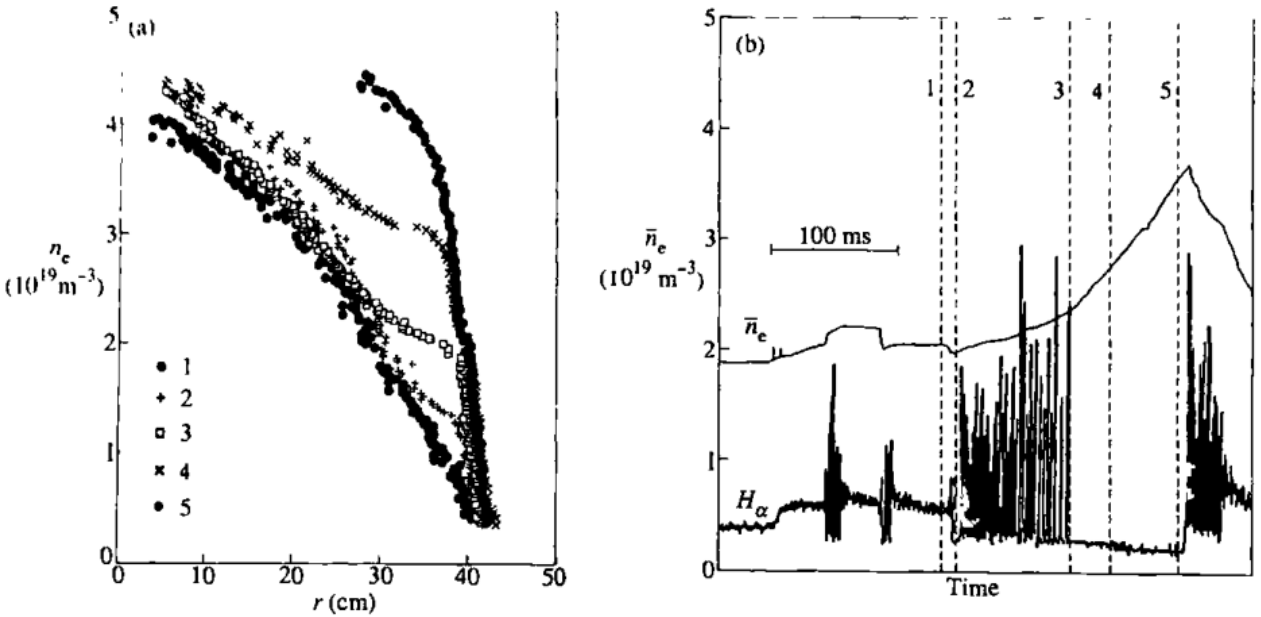

Figure 3: Sequence of density profiles measured on ASDEX through and following an L-H transition. The profiles in (a) are at the times shown in (b), which gives the time dependence of $\bar{n}_e$ and the H_α signal.

Internal Transport Barriers

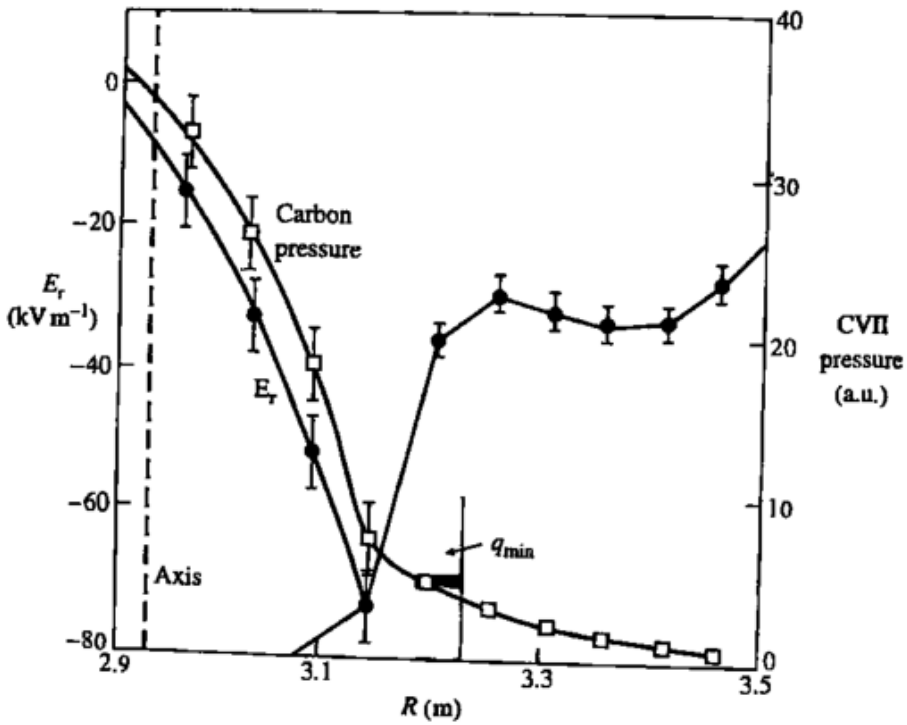

Figure 4: Radial electric field and carbon pressure profiles in an ERS discharge in TFTR. Fluctuations and turbulent fluxes are reduced inside the transport barrier near the minimum in q. Correspondingly, the carbon pressure profile has a stepper gradient in this region. The transport barrier is associated with a rapidly varying profile of E_r.

Outline of Presentation

Fluctuations

- Turbulent fluctuations produce an $\mathbf{E} \times \mathbf{B}$ drift velocity $\delta v_\perp = \delta E_\perp / B$.
- With density fluctuation δn, the convective particle flux is

$$\Gamma = \langle \delta v_\perp \delta n \rangle$$

  Average is taken over the flux surface.
- With magnetic fluctuations $\delta \mathbf{B}$, the flux is

$$\Gamma_j = \frac{n}{B} \langle \delta v_{\parallel j} \delta B_r \rangle$$

Fluctuations and τ_E

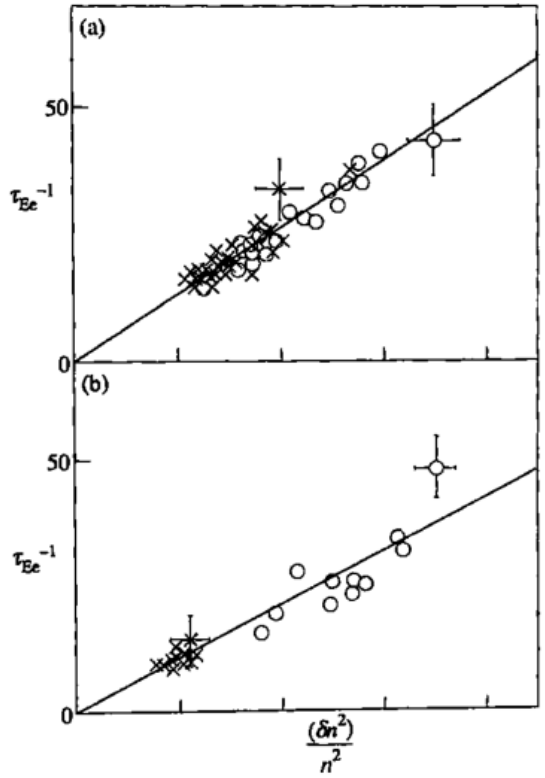

Figure 5: Measurements from TFR showing a correlation between the level of density fluctuations and the electron energy confinement time (with allowance for the effect of sawtooth oscillations). Figure (a) is for ion cyclotron heating and Fig.(b) is for neutral beam beating. Both figures also give results for ohmic heating.

Fluctuations and L-H Transition

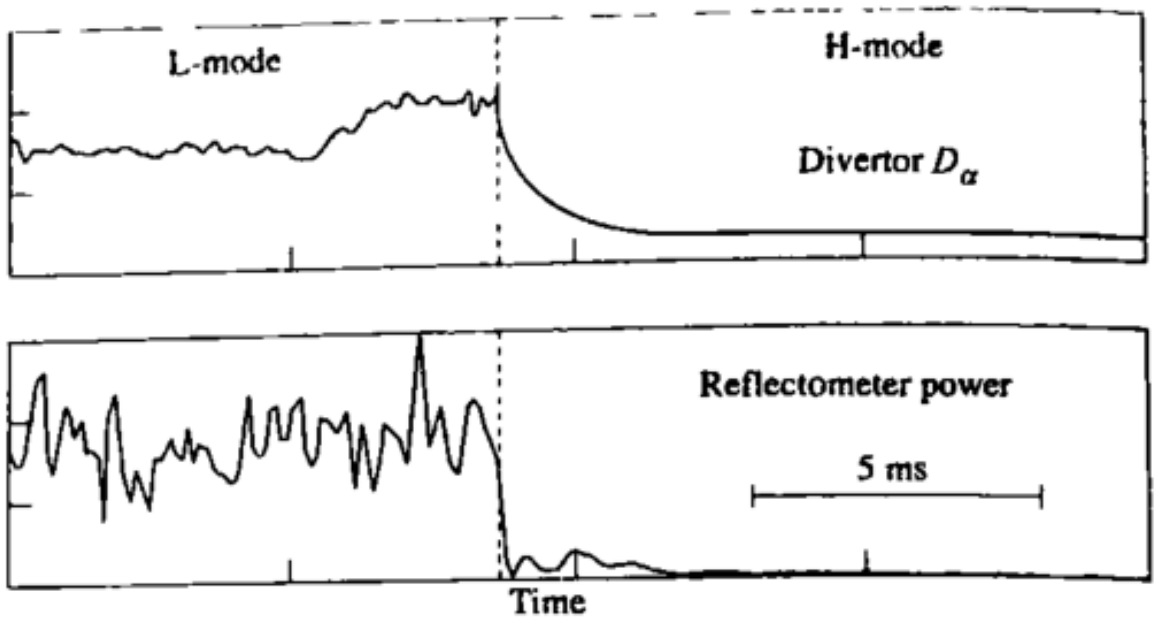

Figure 6: Showing the fall of density fluctuations as measured by reflectometry during an L-H transition in DIII-D.

Turbulence-Induced Transport

- **Transport due to electrostatic fluctuations**:

$$D = \sum_k \left(\frac{k_\perp \delta\phi_k}{B} \right)^2 \tau_k$$

We have assumed the fluctuations of electric potential $\delta\phi = \sum_k \delta\phi_k e^{i\mathbf{k}\cdot\mathbf{x}}$. The time variation of the fluctuation is characterized by $\tau_k \sim 1/\omega_k$.

- **Transport due to magnetic fluctuations**:

$$D_M = \sum_k \frac{k_\perp \omega_k^3}{L_s}$$

All figures are adopted from [4].


F. Chen.
Introduction to Plasma Physics and Controlled Fusion.
Springer, dec 29 2015.


M. Delage, A. Froese, D. Blondal, and D. Richardson.
Progress towards acoustic magnetized target fusion: An overview of the r&d program at general fusion.
In *Canadian Nuclear Society - 33rd Annual Conference of the Canadian Nuclear Society and 36th CNS/CNA Student Conference 2012: Building on Our Past... Building for the Future*, volume 1, pages 285–297, 2012.


M. Laberge.
Experimental results for an acoustic driver for mtf.
Journal of fusion energy, 28(2):179–182, 2009.


J. Wesson and D. J. Campbell.
Tokamaks.
International Monographs on Ph, oct 13 2011.